Durable Anti-Reflective and Anti-Fog Coatings Produced by Aerosol Impact Driven Assembly

Peter Firth[1], Zachary Holman[1], Dave Matthews[1], Ty Newhouse-Illige[1], Ronnie Ramirez[1], and Albert Victoria[1]
Swift Coat, Inc Phoenix, AZ 85029, U.S.A

The Exploration Extravehicular Mobility Unit's (xEMU) helmet is a complex assembly designed to accomplish several tasks to protect and enable astronauts. In addition to maintaining a suitable environment for the wearer, it must also allow for appropriate mobility and provide a wide and undistorted view of the surroundings. A critical component of the helmet's optical system is the anti-fog coating. While previous versions of the anti-fog coating have provided suitable anti-fog performance, they have been difficult to apply, lacked mechanical or chemical durability, or resulted in unanticipated failures (e.g., outgassing of eye-irritating materials during use). This work describes the use of a new coating technology, aerosol impact-driven assembly (AIDA), to develop a next-generation permanent anti-fog coating for the xEMU helmet. AIDA's unique ability to tune both the refractive index and surface roughness of films was used to deposit a thin, transparent (>85% transmittance of visible light), and hydrophilic (contact angle <10°) anti-fog coating. The coating's abrasion resistance and chemical resistance was evaluated and it was found that the coating maintained both its anti-fog and anti-reflective functionally. Finally, the scalability of the process was demonstrated by successfully coating the polycarbonate blanks used to form the helmet's bubble.

Nomenclature

AIDA = Aerosol Impact-Driven Assembly
AFM = Atomic force microscope
AR/AF = Anti-reflective/anti-fog
DI Water = Deionized water
IPA = Isopropanol
n = Refractive index
NASA = National Aeronautics and Space Administration
nm = Nanometers
PECVD = Plasma-enhanced chemical vapor deposition
R_a = Average surface roughness
SEM = Scanning electron microscope
SLM = Standard liters per minute
TMM = Transfer matrix method
xEMU = Exploration extravehicular mobility unit
XPS = X-ray photospectroscopy

I. Introduction

FOGGING occurs when water present in humid air condenses onto a substrate with a temperature at or below the dew point. Droplets on the surface with diameters at least as large as the wavelengths of visible light scatter incident light diffusely, resulting in a hazy image transmitted through the substrate[1]. Depending on the application, the consequences of this condensation-induced haze range from annoying, like a fogged bathroom mirror after a hot shower, to dangerous, like fogged eyewear obscuring vision. The latter is a concern of NASA's spacesuit engineering team, which is pursuing a permanent anti-fog coating for integration into the xEMU spacesuit helmet[2].

[1] Coatings Engineer, Swift Coat, Inc, 2424 W. Desert Cove Ave, Phoenix, AZ

NASA's requirements for an anti-fog coating differ in both intensity and scope from those typical of anti-fog products. In addition to providing exceptional anti-fog functionality, the coating must not reduce total transmittance through the helmet below 70% or increase diffuse transmittance above 3%. Durability is paramount as failure of the coating ends the useful life of an expensive (several thousands of dollars) component that cannot be replaced in the field (i.e., in space or on the lunar surface). The anti-fog coating must operate in the low-pressure spacesuit environment without emitting vapors that may irritate the wearer's eyes or lungs—a problem for previous anti-fog solutions. The coating must also be able to be applied uniformly at a scale large enough to encompass the xEMU helmet, which is approximately 14" in its largest dimension. To date, no commercially available anti-fog product has been able to meet all requirements.

This work details the development of a combination anti-reflective and anti-fog (AR/AF) coating for polycarbonate substrates. Using a novel thin-film deposition technology, Aerosol Impact-Driven Assembly (AIDA), films with unique structures designed to meet NASA's performance requirements for use in the xEMU helmet were produced. The coating's anti-fog performance, optical performance, and durability performance were evaluated. Finally, the ability to produce the AR/AF coating at the functional scale was demonstrated.

II. Background

Strategies to reduce or eliminate fogging typically involve modification of surface energy to produce hydrophilic or hydrophobic surfaces. Hydrophilic surfaces are generally preferred as they do not require an angled surface and gravity to remove water droplets and the materials used to produce hydrophilic surfaces are typically more transparent than those used for hydrophobic surfaces[3].

Many commercially available anti-fog coatings for polycarbonate (e.g., spray solutions) lack mechanical durability and are required to be reapplied regularly, which can result in inconsistent and unpredictable performance. Products from companies like 3M (Scotchgard), FSI (Visgard, Vistex), and NEI (Nanomyte) require a more complex application process (multiple coating steps and curing) but are advertised as "permanent" and provide superior mechanical robustness and longer-lasting performance compared to spray products. 3M, for example, advertises that its Scotchgard product for polycarbonate exhibits a <1% increase in haze after 20 cycles on a Taber linear abraser with a 750g load (the abrasion material and area was not provided) and survives more than 25 wash cycles with deionized (DI) water[4]. NEI's data sheet describes a less than 7% increase in haze after 200 cycles on a Taber rotary abrader with a 500g load using a CS-10F abrasion wheel (~0.5kg/in^2)[5]. Neither company provides data regarding a change in water contact angle after these abrasion tests. While the 3M, FSI, and NEI products represent a distinct improvement compared to spray solutions, their longevity is measured in months. This not acceptable for use in the xEMU helment which is expected to have a useful like of 5+ years.

Recent literature on anti-fog coatings has shifted focus from organic anti-fog coatings like those used by 3M, FSI, and NEI, to composite organic/inorganic and fully inorganic coatings, with SiO_2 being a popular choice for the coating material. SiO_2-based coatings have been found to provide anti-fog behavior equivalent to or better than organic-based coatings and have been shown to have increased abrasion resistance[1].

III. Aerosol Impact-Driven Assembly

A novel approach to producing SiO_2 based anti-fog coatings is Aerosol Impact-Driven Assembly (AIDA), a dry spray process that has demonstrated the ability to produce highly durable super-hydrophilic coatings over large areas at room temperature. The AIDA deposition process is shown in Figure 1.

High flows (several standard liters per minute) of N_2, O_2, and metal-oxide precursors are fed into a plasma reactor where a PECVD-like process is operated at conditions conducive to nucleating nanoparticles. The gas flow drags the nanoparticles downstream where they are accelerated through a slit-shaped nozzle into a roughly evacuated chamber. A substrate is passed through the curtain of particles exiting the slit-shaped nozzle and the particles impact and stick to the substrate to form a thin coating[6, 7]. Deposition occurs at room temperature and no subsequent high-temperature treatments are required, making it compatible with plastic substrates like polycarbonate. No solvents or organic molecules are used in the AIDA deposition process.

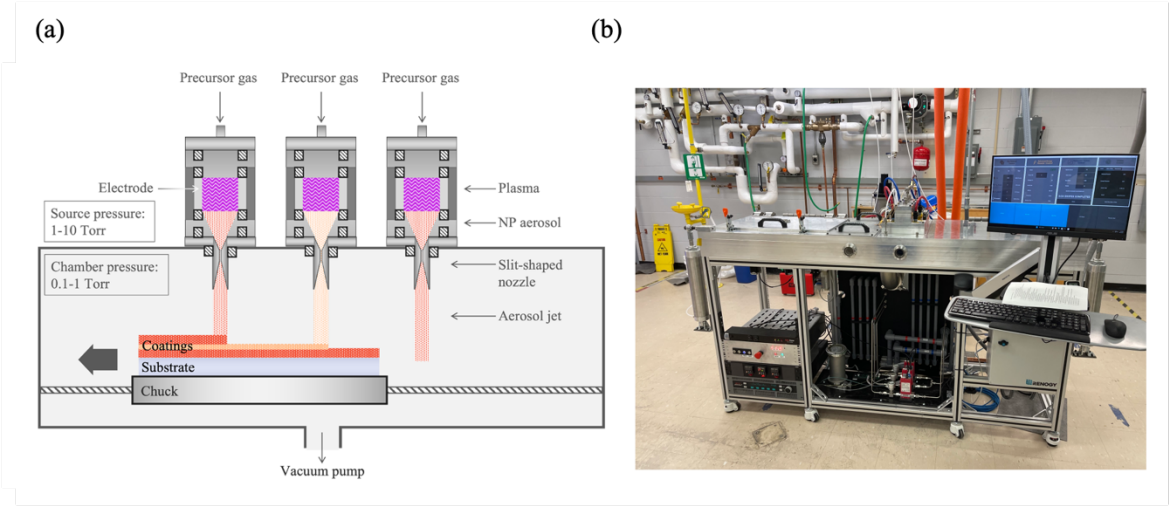

Figure 1. AIDA process overview. *(a) Schematic of an AIDA system equipped with an in-situ plasma reactor for production of nanoparticles. (b) Photograph of a Swift Coat AIDA deposition system capable of coating substrates with dimensions of up to 500mm x 600mm.*

By adjusting process and hardware parameters like chamber pressure, total gas flow, nozzle to substrate distance and nozzle geometry, the particles' impact velocity can be controlled. Control of the particle impact velocity is used to manipulate the deposited coatings' structure—specifically the porosity and surface roughness[6]. SEM cross-sections of films with porosities varying from 97% to 3% and average surface roughness (R_a) varying from 0 nm to 75nm are shown in Figure 2. The size of the pores is small enough and their distribution is uniform enough that the film behaves as an effective medium. The size of the features that make up the rough surface are small enough that wetting behavior is governed by the Wenzel equation. Practically, this means that a change in the film's porosity produces a change in the film's effective refractive index and a change in the film's surface roughness produces a change in the water contact angle [8, 9].

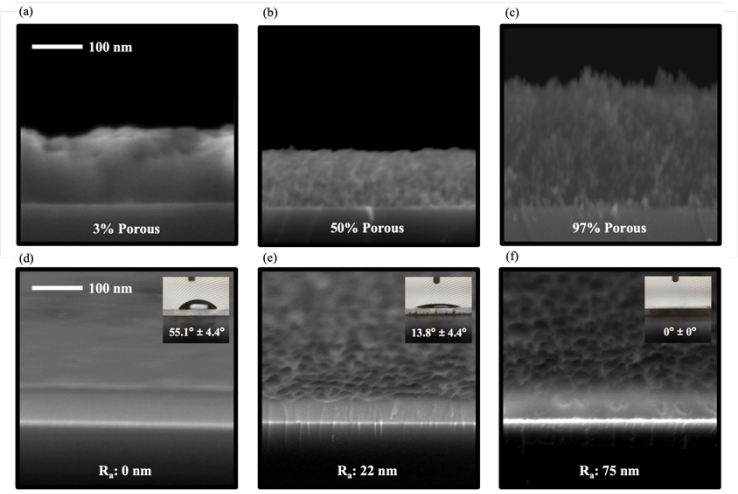

Figure 2. Tunability of films deposited with AIDA. *(a-c) SEM cross-sections of SiO_2 films with varying porosity. (d-f) SEM cross-sections of SiO_2 films with varying surface roughness with corresponding water contact angle images.*

Using AIDA, films composed of SiO_2 nanoparticles were produced. The surface roughness of the films was tuned to produce a super-hydrophilic surface. The porosity was tuned to produce a refractive index that would provide an increase in transmittance (decrease in reflectance) without sacrificing mechanical durability.

IV. Optical Simulations

The interior bubble of the xEMU helmet is made of a Paskolite product, TUFFAK GP. TUFFAK GP is a polished, UV stabilized, high-transparency polycarbonate. At the thickness used in the xEMU helmet (0.27"), TUFFAK GP has a weighted visible light transmittance of ~85%. An acceptable anti-fog coating will not reduce this transmittance

below 70%. An ideal anti-fog coating will provide an increase in transmittance compared to the uncoated substrate. To guide development of the coating, an optical model of the xEMU helmet was built. Using the known achievable refractive index range for films deposited using AIDA, the optical performance (specifically the transmittance and reflectance) of coatings on the helmet was simulated. The results of these simulations guided production of coatings for real-world evaluation.

Transmittance and reflectance measurements of TUFFAK GP were acquired using a Hunterlab Ultra-Scan Pro spectrophotometer with an integrating sphere. The measured reflectance and transmittance spectra can be seen in black in Figure 3 (a) and (b), respectively. Ellipsometry measurements of TUFFAK GP were taken with a JA Woollam M-2000 variable angle spectroscopic ellipsometer. Using JA Woollam's CompleteEase software, a Cauchy Model for the optical constants was simultaneously fit to the reflectance, transmittance, and ellipsometry data in the transparent region of the substrate (500nm – 1000nm). The optical constants determined from the Cauchy Model were then used as a first guess in a more complex B-Spline model. The B-Spline model was used to capture absorption in the substrate. The Transfer Matrix Method (TMM) was then used with the optical constants determined by the B-Spline model to simulate reflectance and transmittance spectra for the TUFFAK GP. The simulated spectra are shown in red in Figure 3 (a) and (b). The simulated spectra match both the shape and intensity of the measured spectra, confirming that the simulation methodology can be used to predict real-world performance.

To identify coating structures that would produce the desired optical performance, 600 unique coating structures were simulated. Each structure consisted of a 10 nm thick binding layer (composed of a proprietary, inorganic material also deposited by AIDA) and a theoretical anti-fog layer of variable thickness and refractive index. A diagram of the simulated structures is shown in Figure 4 (a). The results of these simulations are summarized in Figure 4 (b). Figure 4 (b) plots the weighted transmittance for various thickness and refractive index combinations of the anti-fog layer. The plot indicates that nearly all simulated structures result in a weighted transmittance greater than 70% and that a wide range of structures result in transmittance greater than 85%. Based on our previous experience with AIDA SiO_2 coatings, structures with refractive indexes between 1.25 and 1.35 were selected. The data in Figure 4(b) suggests that films with these refractive indexes can result in a 2-5% increase in transmittance compared to bare polycarbonate.

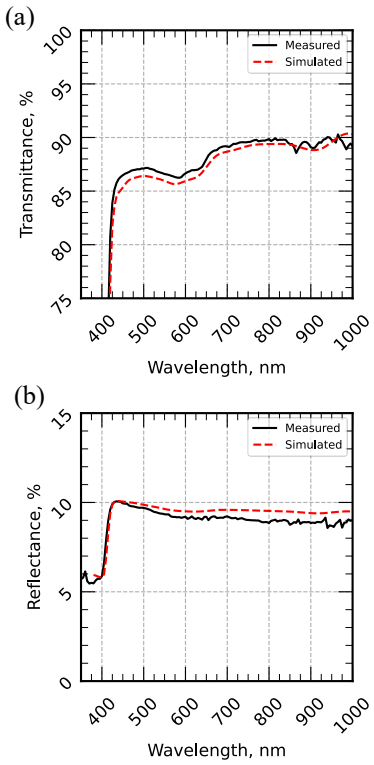

Figure 3. Optical model of the xEMU helmet. *(a) Transmittance spectra of measured (black) and simulated (red) TUFFAK GP polycarbonate. (b) Reflectance spectra of measured (black) and simulated (red) TUFFAK GP polycarbonate.*

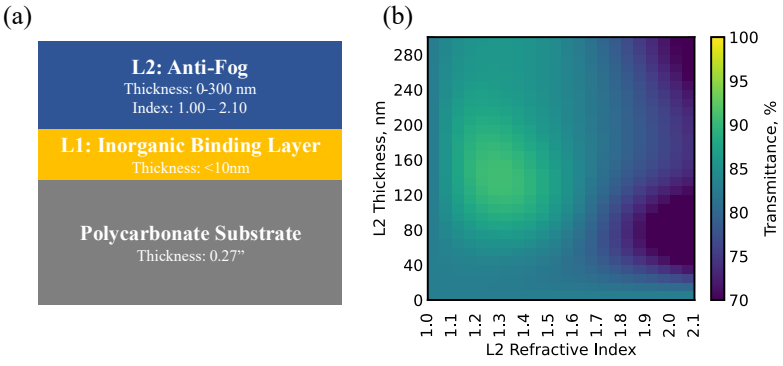

Figure 4. Simulated performance of AIDA anti-fog coatings on polycarbonate substrates. *(a) Diagram of the simulated structure. The properties of the polycarbonate substrate and inorganic binding layer were held constant while the thickness and index of the anti-fog layer were varied (b) Summary of simulation results. Nearly all simulated structures resulted in a transmittance higher than 70%.*

This range of refractive indexes corresponds to film porosities between 20% and 40%, and such AIDA films are known to exhibit good mechanical durability.

V. Characterization of Fabricated Coatins

Using the simulations described in the previous section as a guide, coatings with a range of refractive indexes and thicknesses were fabricated. Two champion samples are presented in Figures 5 and 6: one with a low average surface roughness (low R_a) and one with a high average surface roughness (high R_a). Figure 5 (a) and (b) map the topography of the low-R_a and high-R_a AR/AF coatings. These data were collected using an atomic force microscope (AFM). The AFM data reveals that the low-R_a coating had an average surface roughness of 10 nm and that the high-R_a coating had an average surface roughness of 75 nm. Figure 5 (c) shows the reflectance spectra of polycarbonate substrates coated with the low-R_a and high-R_a AR/AF coatings. Both coatings provide a reduction in reflection compared to uncoated polycarbonate. The surface roughness of the high-R_a coating produces a flatter spectrum, resulting in a more color-neutral appearance.

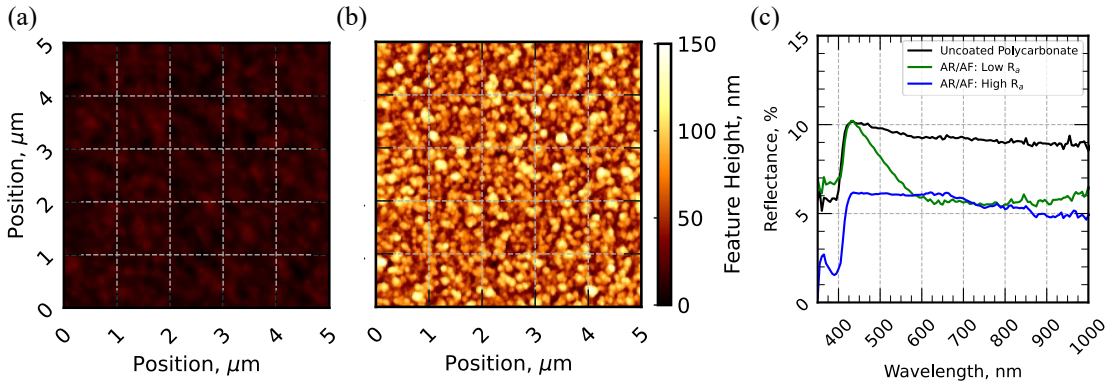

Figure 5. Characterization of AR/AF coatings. *(a) Topography of a low-R_a AR/AF coating collected using AFM. The data indicate an average surface roughness of approximately 10 nm. (b) Topography of a high-R_a AR/AF coating collected using AFM. The data indicate an average surface roughness of approximately 75 nm. (c) Reflectance spectra of the low (green) and high (blue) R_a AR/AF films.*

The anti-fog functionality of the coatings was evaluated using the "coffee cup test" and contact angle measurements. The coffee cup test consists of placing a room temperature sample on top of a vessel (e.g., a coffee cup) containing hot (nominally 90°C) water. Samples remain on top of the vessel for approximately 30 seconds as hot water vapor condenses on the cooler sample surface. A photograph of a samples in this state is evaluated by eye to provide a mostly subjective evaluation of anti-fog performance. Contact angle measurements were performed using a VCA Optima XE contact angle system. Figure 6 summarizes the anti-fog performance of the high- and low-R_a AR/AF coatings.

Figure 6 (a), (b) and (c) are photographs of uncoated polycarbonate, polycarbonate coated with the low-R_a AR/AF coating, and polycarbonate coated with the high-R_a AR/AF coating undergoing the coffee cup test. Inset in each image is the water contact angle. Both versions of the anti-fog coating result in a lower contact angle than uncoated polycarbonate. The low-R_a coating has a contact angle of approximately 6° while the high-R_a coating's contact angle is near zero. Performance on the coffee cup test correlates well with the contact angle measurements. The uncoated polycarbonate fogs quickly, resulting in significantly reduced visibility of the text at the bottom of the cup. The low-R_a coating provides significantly better visibility of the text at the bottom of the cup, though the text is distorted and difficult to read. The high-R_a coating performs best on the coffee cup test, resulting in text that is both visible and undistorted.

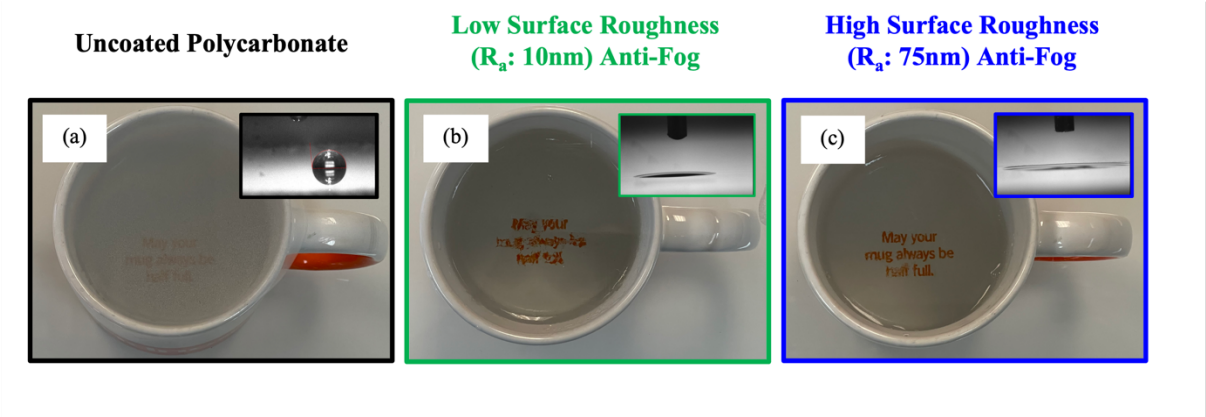

Figure 6. Anti-fog performance of AR/AF films. *(a) Photograph of uncoated polycarbonate substrate undergoing the coffee cup test. The sample quickly fogs resulting in the text at the bottom of the cup becoming dim and hazy. The inset image shows a contact angle of 70° degrees. (b) Photograph of a polycarbonate substrate with the low-R_a coating undergoing the coffee cup test. Fogging is clearly less than the uncoated case, but some distortion of the text is noted. The inset image shows a contact angle of 6°. (c) Photograph of a polycarbonate substrate with the high-R_a coating undergoing the coffee cup test. There is nearly no visible fogging. The inset image shows a contact angle of near 0°.*

VI. Durability

As the high-R_a AR/AF coating had superior optical properties and anti-fog performance, it was selected to undergo durability testing. To evaluate the coating's abrasion resistance, a Taber linear abrasion system (Model 5750) was utilized. Damp cheese cloth was selected as the abrasive material with 3lb/in^2 of normal pressure applied to the 2"x4" substrate. The sample was subjected to 250 abrasion cycles at a rate of 60 cycles per minute. Figure 7 summarizes the results of this test.

Figure 7 (a) contains reflectance spectra of uncoated polycarbonate (black) and polycarbonate with the high-R_a AR/AF coating before and after abrasion testing. The post-abrasion reflectance spectrum matches the shape and intensity of the as-deposited spectrum, indicating minimal change to the coating structure. Figure 7 (b) and (c) are water contact angle images before and after abrasion testing, respectively. Both contact angles are near 0°, indicating the anti-fog functionality is intact. These results suggest that the AR/AF coating's optical and anti-fog performance will be maintained after light to moderate scrubbing.

The coating's abrasion resistance can be partially understood by examining its structure. Figure 7 (d) and (e) are SEM images of the sample before and after abrasion testing, respectively. The large image is a 5,000X magnification, top-down view of the sample's surface. The inset

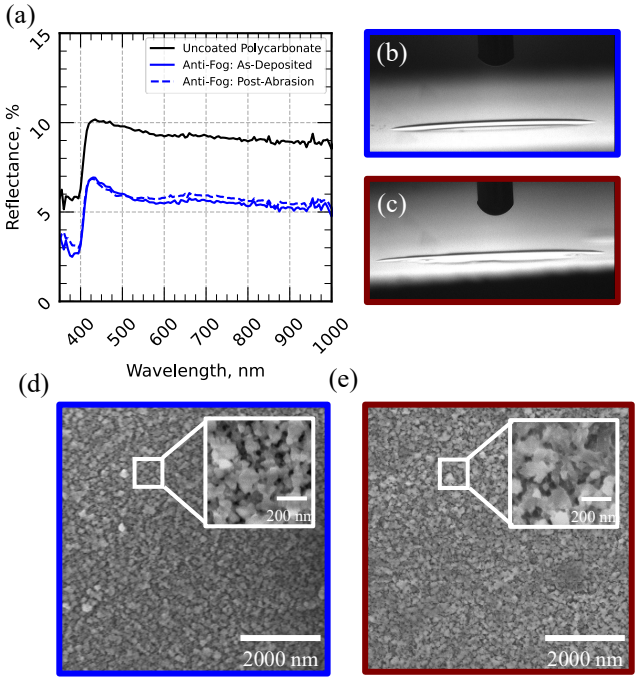

Figure 7: Mechanical durability of high R_a AR/AF coating. *(a) Reflectance spectra before and after abrasion testing. (b) Contact angle measurement before abrasion testing. (c) Contact angle measurement after abrasion testing. (d) Top-down SEM image of the sample before abrasion testing. (e) Top-down SEM image of the sample after abrasion testing.*

image is a 50,000X magnification top-down view of the sample's surface. The SEM images show significant interconnection (often referred to as "necking") between particles. This extensive necking immobilizes the material resulting in a more durable film.

To evaluate the coatings' resilience to cleaning agents, the high-R_a AR/AF coating was soaked in four common cleaning solutions: (1) DI water, (2) DI water with detergent, (3) isopropanol (IPA), and (4) Windex. Samples were submerged in the solutions for a total of 24 hours. After the soaks were complete, the samples were removed, rinsed with DI water, and blown dry with compressed nitrogen. Figure 8 summarizes the results of this test.

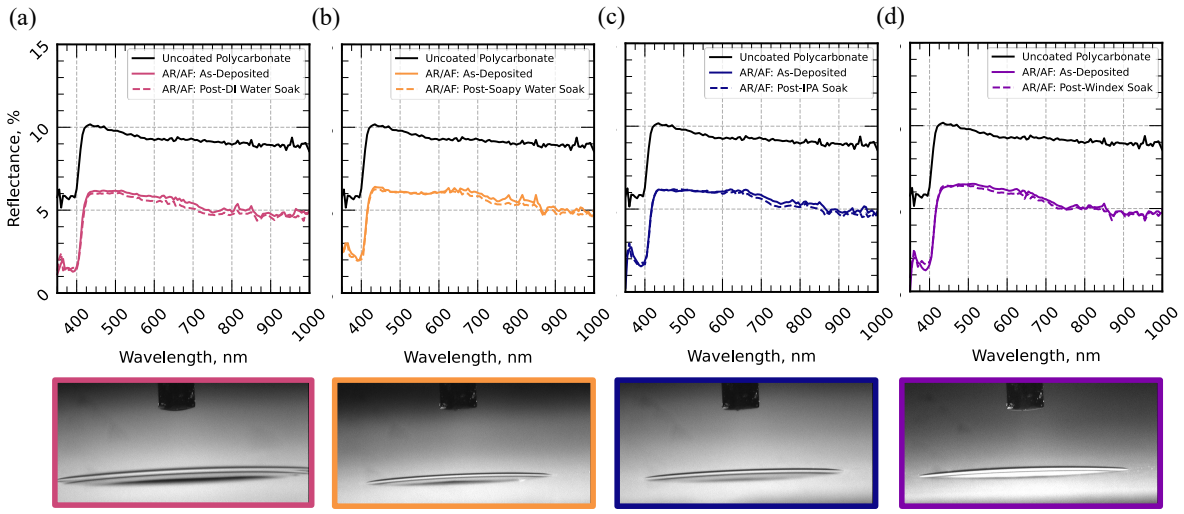

Figure 8. Results of 24-hour chemical soak tests. *Reflectance spectra of high-R_a AR/AF coated polycarbonate before (solid) and after (dashed) soaking in (a) DI water, (b) DI water with detergent, (c) isopropanol, and (d) Windex for 24 hours. Below each plot are contact angle measurements of each sample after completion of the soak tests.*

Figure 8 (a) - (d) contain reflectance spectra before and after chemical soak testing. Below each reflectance plot is the post-test water contact angle measurement. In all cases, the post-test reflectance spectra match the shape and intensity of the pre-test reflectance spectra, indicating minimal change to the coating's structure. The post-test contact angle for all tests remained near 0°, indicating the anti-fog functionality is intact.

The coating's resilience to the tested cleaning agents can be explained by its composition. Figure 9 is an X-ray photoelectron spectroscopy (XPS) spectrum of the high-R_a AR/AF film. The spectrum shows only three peaks: (1) a peak at 99 eV representing the 2p binding energy for silicon, (2) a peak at 151 eV representing the 2s binding energy for silicon, and (3) a peak at 533 eV representing the 1s binding energy of oxygen[10]. The spectrum suggests that the film is composed of very pure SiO_2, a generally unreactive material.

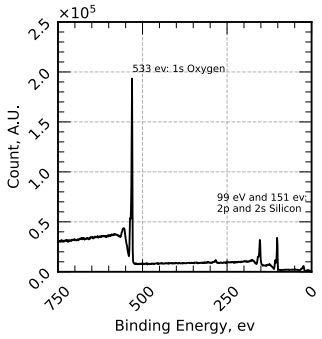

Figure 9: Chemical composition of AR/AF coating. *XPS spectra of the high-R_a AR/AF film. The spectrum shows peaks for oxygen and silicon, indicating the film is composed of very pure SiO_2.*

VII. Scaling

For use in the xEMU helmet, the AR/AF coating would need to be applied to an area approximately 14" x 11". To accomplish this, the AR/AF deposition process was transitioned to an AIDA deposition system capable of coating substrates up to 19.5" wide. A photograph of the system can be seen in Figure 1 (b). As an initial test, the high-R_a AR/AF coating was deposited on a flat 12" x 12" polycarbonate substrate. To evaluate non-uniformity, 15 reflectance measurements were taken in an equally spaced 5 x 5 grid pattern. A plot of weighted reflectance as a function of position is shown in Figure 10 (a). The average weighted reflectance of the

sample was 6.03% ± 0.29%, representing a non-uniformity of 7.5%. Figure 10 (b) and (c) are photographs of 12” x 12” uncoated and AR/AFcoated polycarbonate samples undergoing a modified version of the coffee cup test. In this version of the test, the temperature of the water bath was 50°C rather than 90°C due to limitations of the vessel. Consistent with the results of the small-scale tests, the AR/AF coating significantly reduces fogging.

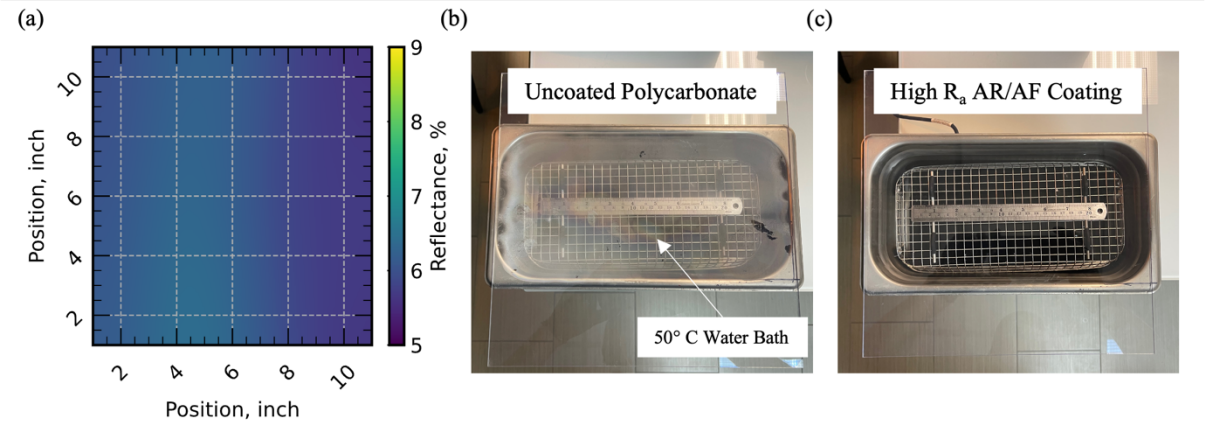

Figure 10: Scaling the AR/AF coating to 12” x 12” substrates. *(a) Map of weighted reflectance produced from 25 reflectance measurements taken in a 5x5 grid on a 12” x 12” polycarbonate sample. (b) Photograph of a 12” x 12” uncoated polycarbonate substrate undergoing a scaled up version of the coffee cup test. (c) Photograph of a 12” x 12” AR/AF coated polycarbonate substrate undergoing a scaled up version of the coffee cup test.*

The unique challenge with applying this (or any) coating to the xEMU helmet is its hemi-elippsoidal shape. There are two approaches. The first is applying the coating to a flat polycarbonate sheet before it is formed into the final shape. This would require the coating be able to survive the forming process. The second is applying the coating to the finished part. This would require that the coating process be capable of applying the coating uniformily to a curved substrate. Initial experiments were conducted to evaluate the feasibily of both approaches.

The feasibility of coating a pre-formed part is summarized in Figure 11 and Figure 12. Figure 11 (a) and Figure 11 (b) are photographs of a flat polycarbonate substrate with and without the AR/AF coating after undergoing the modified version of the coffeecup test, respectively. As expected, the uncoated part shows significant fogging while the coated part remains clear. The polycarbonate substrate was procured from the xEMU helmet manufacturer and cut to the appropriate shape for forming before the AR/AF coating was applied. Figure 11(c) plots the reflectance spectra of the uncoated polycarbonate (black) and the AR/AF coated polycarbonate (purple). The dashed purple line

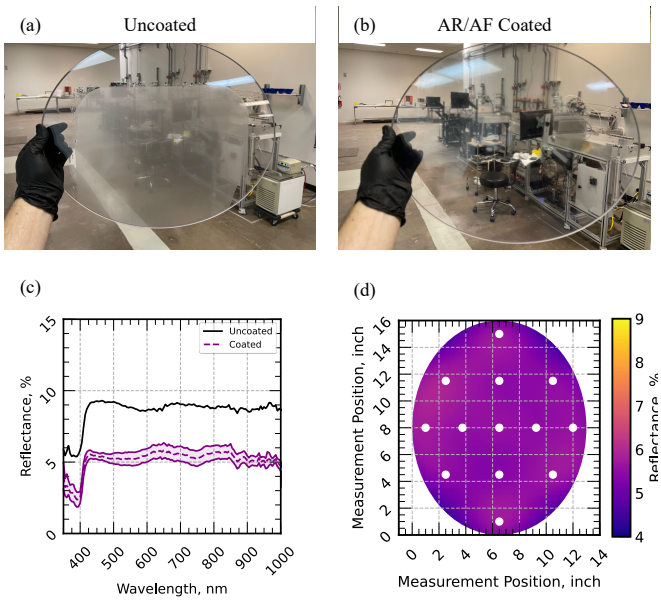

Figure 11: Feasibility of producing a ‘formable’ coating *(a),(b) Photographs of uncoated and coated flat polycarbonate sheets procured from the xEMU helmet manufacture after fog testing, respectively. The coated sample shows no obvious fogging. . (c) Average (dashed purple) reflectance spectrum and 95% confidence interval (purple shaded region) of 13 points measured across the coated sample. (d) Map of weighted reflectance measurements taken on the coated sample.*

represents the average reflectance and the shaded area represents the 95% confidence interval for 13 points measured at various locations on the susbtrates. Figure 11(d) is a map of the weighted reflectance of the coated sample. The white dots represent the measurement locations. The fogging behavior, spectrum shape, and spectrum intensity are consistant with previous results.

The coated substrate shown in Figure 11 was subsequently formed into the required shape for the xEMU helmet by the helmet manufacturer using a proprietary process. The initial evaluation of this part is summarized in Figure 12. Figure 12 (a) is a photograph of the helmet formed from the coated polycarbonate sheet shown in Figure 11. The manufacture did not note any issues with using a coated part. The only visual defect in the helmet is a light haziness. To evaluate if the coating survived the forming process, reflectance measurements of the coated interior and the uncoated exterior were taken usng a Filmetrics F20-UV spectrophotometer with a contact probe designed to measure reflectance of curved surfaces. The probe is designed such that only reflectance from the surface in contact with the probe is measured (i.e. light reflected off the backside is not captured). The reflectance spectra of the uncoated exterior and the coated interior are shown in Figure 12 (b). The reflectance of the coated interior is approximately 2.5% lower than the exterior indicating that the AR/AF coating is still present on the interior surface.

To test the feasibily of coated a curved part, a plastic cup with a diameter of three inches and a height of two inches (largest height that can fit in the current AIDA reactor) was coated with the AR/AF coating. Figure 13 contains photographs of the coated and an uncoated cup undergoing the coffee cup test. It can be clearly sseen that the entirety of the cup's interior has been coated as no fog build up is evident.

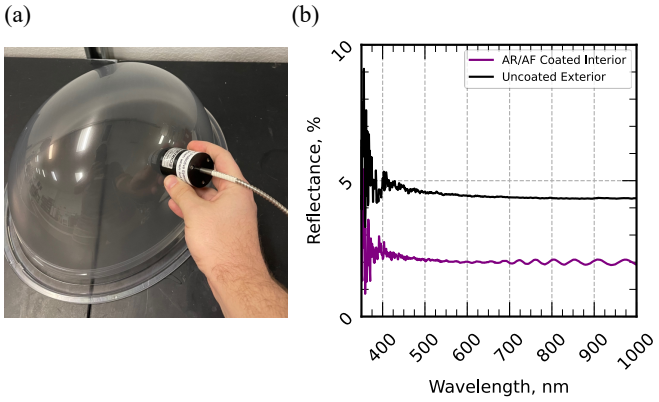

Figure 12: Performance of coated xEMU helmet. *Using the coated susbtrate shown in Figure 11, an xEMU helmet was produced. (a) Photograph of the helmet undergoing a reflectance measurement. The helmet had a slight hazy appearance. (b) Reflectance spectra of the helmet's uncoated exterior (black) and coated interior (purple). The coated interior has ~2.5% lower reflectance than the uncoated exterior surface.*

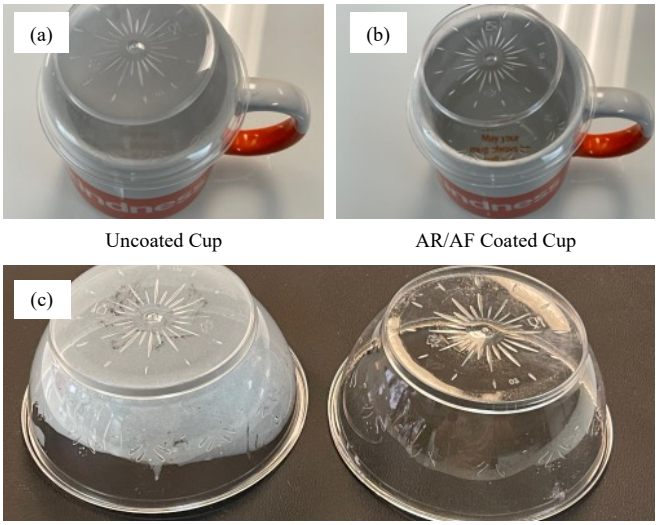

Figure 13: Deposition of AR/AF coatings onto curved parts. *(a),(b) Photographs of a plastic cup and a plastic cup coated with the AR/AF coating undergoing the coffee cup test. The text at the bottom of the mug is clearly visible through the coated cup and obscured by fog on the uncoated cup. (c) Photograph of the uncoated (left) and coated (right) cups after removal from the coffee cup test and placed against a black background for improved visibility.*

VIII. Future Work and Opportunities

Both approaches to applying the AR/AF coating to the xEMU helmet seem viable from initial experimention, though many challenges remain. Coating a flat part that is later formed into a helmet is considerably easier from a manufacturing perspective, but the hazy appearance of the first helmet will need to be diagnosed and rectified. Succesffuly coating the plastic cup with steep sidewalls suggests that with proper hardware the coating could be applied to the

finished xEMU helmet, but this hardware would need to be developed and optimized for this process. Future work will include evaluating, optimizing, and ultimately down-selecting to one of these approaches.

Future work will also include additional UV exposure, thermocycling, low-earth-orbit environment exposure, spit/sweat/vomit exposure, and scratch resistance to provide a full evaluation of the coatings performance in relevant environments.

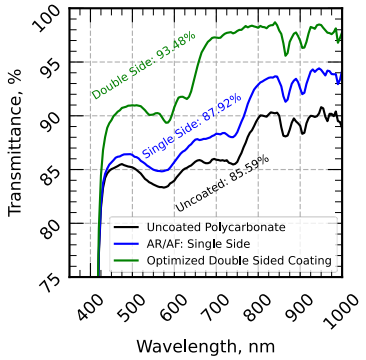

Figure 14 Double-Sided Coatings. *Transmittance spectra of uncoated polycarbonate (black), polycarbonate coated with the high-R_a AR/AF coating (blue) on one side, and polycarbonate coated on both sides with a version of the AR/AF coating designed to maximize transmittance.*

The initial scope of this work included application of an anti-fog coating only to the most interior surface of the xEMU helmet. As the coating's optimized structre resulted an increase in transmittance while maintaining durability, there are opportunities to coat other surfaces within the xEMU helmet and provide an additional increase in transmittance. In total, there are six polycarbonate/air interfaces present in the helmet. If all surfaces are uncoated, this will result in a total transmittance between 60 and 70%. A version of the AR/AF coating developed in this work could be applied to every polycarbonate/air surface in the helmet, increasing the total transmittance by as much as 25%. As a proof of concept, the design of the AR/AF coating was optimized to maximize transmittance if applied to both sides of a polycarbonate substrate. The transmittance spectrum of this coating is shown in Figure 14. The double-sided coated substrate had 7.89% higher transmittance compared to an uncoated polycarbonate substrate.

IX. Conclusion

In this work, it was demonstrated the production of a combination anti-fog, anti-reflective coating for polycarbonate substrates produced using Aerosol Impact-Driven Assembly. By optimizing the surface roughness, thickness, and porosity, a coating was produced that was super-hydrophilic, provided a 2-3% increase in transmittance, and maintained functionality after abrasion testing and chemical soak tests. The scalability of the manufacturing process was demonstrated by producing coatings on 12" x 12" flat substrates, a full scale helmet, and curved samples that provided the desired anti-fog and anti-reflective performance. Finally, it was shown that small tweaks to the structure of the coating could make it useful in other aspects of the xEMU helmet, specifically as an anti-reflective coating applied to each polycarbonate/air interface to significantly increase light transmittance.

Acknowledgments

We acknowledge the use of facilities within the Eyring Materials Center at Arizona State University supported in part by NNCI-ECCS-1542160.

References

1. Duran, I.R. and G. Laroche, *Current trends, challenges, and perspectives of anti-fogging technology: Surface and material design, fabrication strategies, and beyond.* Progress in Materials Science, 2019. **99**: p. 106-186.
2. Davis, K. and G. Trude. *Exploration Helmet Permanent Anti-Fog Study*. in *52nd International Conference on Environmental Systems (ICES)*. 2023.
3. Wahab, I.F., et al., *Fundamentals of antifogging strategies, coating techniques and properties of Inorganic materials; a comprehensive review.* Journal of Materials Research and Technology, 2023.
4. *3M Scotchgard Anti-Fog Technology*. [cited 2023; Available from: https://multimedia.3m.com/mws/media/1383834O/3m-securefit-600-technology.pdf.
5. Corporation, N. *NANOMYTE® SAF-200 Technical Data sheet*. 2020 [cited 2023 03/13/2023]; Available from: https://neicorporation.com/tds/NANOMYTE_SAF-200_TDS.pdf.
6. Firth, P. and Z.C. Holman, *Aerosol Impaction-Driven Assembly System for the Production of Uniform Nanoparticle Thin Films with Independently Tunable Thickness and Porosity.* ACS Applied Nano Materials, 2018. **1**(8): p. 4351-4357.
7. Firth, P.A. and Z. Holman, *System and methods for deposition spray of particulate coatings*. 2018, US Patent App. 15/611,627.

8. Vulic, N., et al., *Pore formation in silicon nanoparticle thin films and its impact on optical properties.* ACS Applied Energy Materials, 2019. **2**(12): p. 8587-8595.
9. Whyman, G., E. Bormashenko, and T. Stein, *The rigorous derivation of Young, Cassie–Baxter and Wenzel equations and the analysis of the contact angle hysteresis phenomenon.* Chemical Physics Letters, 2008. **450**(4-6): p. 355-359.
10. Chastain, J. and R.C. King Jr, *Handbook of X-ray photoelectron spectroscopy.* Perkin-Elmer Corporation, 1992. **40**: p. 221.